

# APVR: Hour-Level Long Video Understanding with Adaptive Pivot Visual Information Retrieval

Hong Gao<sup>1,2\*</sup>, Yiming Bao<sup>2\*</sup>, Xuezhen Tu<sup>2</sup>, Bin Zhong<sup>2</sup>, Minling Zhang<sup>1†</sup>

<sup>1</sup>SouthEast University, <sup>2</sup>ZTE Corporation

## Abstract

Current video-based multimodal large language models struggle with hour-level video understanding due to computational constraints and inefficient information extraction from extensive temporal sequences. We propose APVR (Adaptive Pivot Visual information Retrieval), a training-free framework that addresses the memory wall limitation through hierarchical visual information retrieval. APVR operates via two complementary components: Pivot Frame Retrieval employs semantic expansion and multi-modal confidence scoring to identify semantically relevant video frames, while Pivot Token Retrieval performs query-aware attention-driven token selection within the pivot frames. This dual granularity approach enables processing of hour-long videos while maintaining semantic fidelity. Experimental validation on LongVideoBench and VideoMME demonstrates significant performance improvements, establishing state-of-the-art results for not only training-free but also training-based approaches while providing plug-and-play integration capability with existing MLLM architectures.

## 1 Introduction

The proliferation of long-form video content necessitates robust understanding capabilities that extend beyond the current limitations of video-based multimodal large language models. While exist models (Lin et al. 2023; Zhang et al. 2025) demonstrate proficiency on short video sequences, they encounter fundamental scalability challenges when processing hour-level content, where the quadratic complexity of attention mechanisms creates prohibitive computational demands and semantic information becomes diluted across extensive temporal spans.

The core challenge stems from the inability of current Video MLLMs to effectively model and extract critical information from long video sequences. In hour-level videos, semantically relevant content typically represents a sparse subset of the total temporal sequence, yet existing approaches process entire sequences by uniform sampling, leading to computational inefficiency and degraded performance due to attention dispersion across irrelevant segments.

Contemporary approaches to long video understanding bifurcate into training-based and training-free paradigms, each presenting distinct limitations that constrain practical deployment. Training-based methods employ strategies such as multimodal sequence parallelism (Fu et al. 2025; Liu et al. 2024d) or compression techniques (Shu et al. 2024; Liu et al. 2025a) during the training phase to accommodate extended sequences. However, these approaches suffer from several critical drawbacks that limit their applicability. First, they require substantial training datasets and computational resources, making them prohibitively expensive for many new scenes. Second, the long-video training process often compromises the model’s foundational capabilities on shorter sequences, necessitating replay training to maintain performance across diverse sequence lengths. Third, these methods exhibit poor adaptability when confronted with novel task distributions that differ significantly from their training domains, requiring extensive retraining or fine-tuning procedures.

Training-free methods present an alternative paradigm focused on keyframe retrieval and selective processing strategies (Tang et al. 2025a; Cheng et al. 2025a; Luo et al. 2025). While these approaches offer computational advantages and deployment flexibility, they face fundamental limitations in their current implementations. Existing keyframe retrieval methods typically select only a limited number of video frames, which proves insufficient for tasks requiring comprehensive temporal reasoning and long-range logical understanding. Furthermore, when researchers attempt to increase the number of selected frames to improve coverage, these methods quickly encounter out-of-memory limitations, effectively hitting the memory wall that prevents processing of truly long sequences. The trade-off between sequence coverage and computational feasibility has prevented existing training-free methods from achieving the temporal comprehensiveness necessary for complex video understanding tasks.

Our proposed Adaptive Pivot Visual information Retrieval (APVR) framework addresses these limitations through a novel training-free approach that combines strategic keyframe retrieval with adaptive token selection and compression mechanisms. Our approach is motivated by the observation that effective long video understanding requires strategic information retrieval at multiple gran-

\*Equal Contribution

†Corresponding Author

ularities. Rather than processing entire video sequences uniformly, APVR employs a two-stage retrieval mechanism that operates at both frame and token levels to identify and extract pivot visual information that is most relevant to the input query. This dual granularity strategy enables the system to breakthrough the memory wall while maintaining semantic accuracy across long video understanding tasks. By focusing computational resources on the most semantically relevant frames and subsequently performing intelligent token compression within those frames, APVR achieves comprehensive coverage of hour-long videos without encountering memory limitations.

The core innovation of APVR lies in its adaptive retrieval strategy that combines semantic information expansion with multi-modal confidence scoring. At the frame level, our **Pivot Frame Retrieval (PFR)** component expands the original query into four types of semantic information: *objects, descriptions, relations, and semantics*. This expansion enables more comprehensive frame scoring using complementary visual models, specifically CLIP for semantic similarity and Grounding-DINO for object detection and spatial reasoning. The framework incorporates temporal diffusion mechanisms to maintain temporal coherence and employs adaptive resampling strategies to progressively refine frame selection across multiple iterations. At the token level, our **Pivot Token Retrieval (PTR)** component extends the concept of semantic importance to fine-grained visual representations. This component leverages query-aware multi-layer attention scoring to identify the most relevant visual tokens within selected frames, employing dynamic chunk-wise selection and head-wise soft voting mechanisms to maintain both computational efficiency and semantic accuracy.

The main contributions of this work are summarized as follows:

- We propose APVR, a novel training-free framework that addresses scalability challenges in long video understanding through dual-granularity information retrieval. Our approach combines frame-level pivot retrieval with token-level adaptive selection to breakthrough the memory wall.
- We develop a mechanism that leverages multi-modal confidence scoring and query-aware attention scoring to preserve temporal structure and semantic details, ensuring accurate understanding of complex video narratives while maintaining computational efficiency.
- We demonstrate that intelligent multi-granularity retrieval provides a sustainable alternative to parameter scaling for long video understanding. Our training-free design ensures plug-and-play integration with existing MLLM architectures while preserving foundational capabilities.

## 2 Related Work

**Video MLLMs** Recent years have witnessed significant advances in multimodal large language models (MLLMs) for visual perception and understanding. As a critical modality in visual data analysis, video has also been integrated into MLLM frameworks. Notable efforts include Qwen2.5-VL (Bai et al. 2025a), InternVideo2.5 (Wang et al. 2025b), VideoLlama3 (Zhang et al. 2025), and VideoChat-Flash (Li et al. 2024b), which explore video understanding through a

unified architecture consisting of three key components: (a) a video encoder for spatio-temporal feature extraction, (b) a projector for aligning visual features with linguistic embeddings, and (c) a video-aware LLM for multimodal reasoning. Due to the inherent complexity of video content (e.g., multi-object interactions, long-range temporal dependencies), existing MLLMs often fail to extract semantically salient information for video-centric downstream tasks requiring precise spatiotemporal reasoning, such as video question answering and spatiotemporal video grounding. Some works (Bai et al. 2025a; Wei et al. 2025) exploit to aggregate timestamps in the RoPE (Su et al. 2024). However, these methods exhibit significant performance degradation when extrapolating to videos exceeding their pre-training duration. Moreover, current architectures also exhibit limitations of inefficient cross-modal alignment between visual information and linguistic queries, particularly in long-form videos exceeding 5 minutes (Li et al. 2024a).

**Long Video Understanding** Recently advances in long video understanding can be broadly categorized into training-based and training-free paradigms. In the training-based paradigm, MLLMs are directly trained using large-scale long video datasets. The whole training process is usually divided into several stages to stably improve different components of MLLM, as well as to improve the ability to model different types of input visual data (Li et al. 2024b; Zhang et al. 2025). In order to process extra-long videos, current methods explore two different strategies: sequence parallelism (Chen et al. 2024; Zhang et al. 2024b; Shen et al. 2025) or visual feature compression (Song et al. 2024; Shen et al. 2024; Liu et al. 2025a). For instance, LongVILA (Chen et al. 2024) adopts a five-stage training pipeline with a novel multi-modal sequence parallelism to efficiently understand long videos. Video-XL-Pro (Liu et al. 2025a) builds a learnable module to generate compact and comprehensive video tokens for hour-long video understanding. In the training-free paradigm, long video understanding task is organized as an agent-like process (Liu et al. 2025b; Wang et al. 2024c), where MLLMs serve as reasoning engine within the system. These training-free methods mainly focus on retrieving the most important information in video frames (Tang et al. 2025b; Park et al. 2024; Ye et al. 2025; Guo et al. 2025; Cheng et al. 2025b) or visual tokens (Wang et al. 2025a; Luo et al. 2025). For example, AKS (Tang et al. 2025b) adopts a plug-and-play module for keyframe selection and information pre-filtering for video-based MLLMs. QuoTA (Luo et al. 2025) adopts an ante-hoc training-free modular for query-aware visual token assignment and important information retrieval. Despite these advancements, few methods simultaneously explore frame and token optimization, which is addressed in this work through adaptive pivot information retrieval.

## 3 Method

### 3.1 Overview

The framework of the proposed APVR is illustrated in Fig. 1, which is a training-free system. Given an input video  $\mathcal{F} = \{f_t\}_{t=1}^N$  with  $N$  frames and query  $Q$ , the system

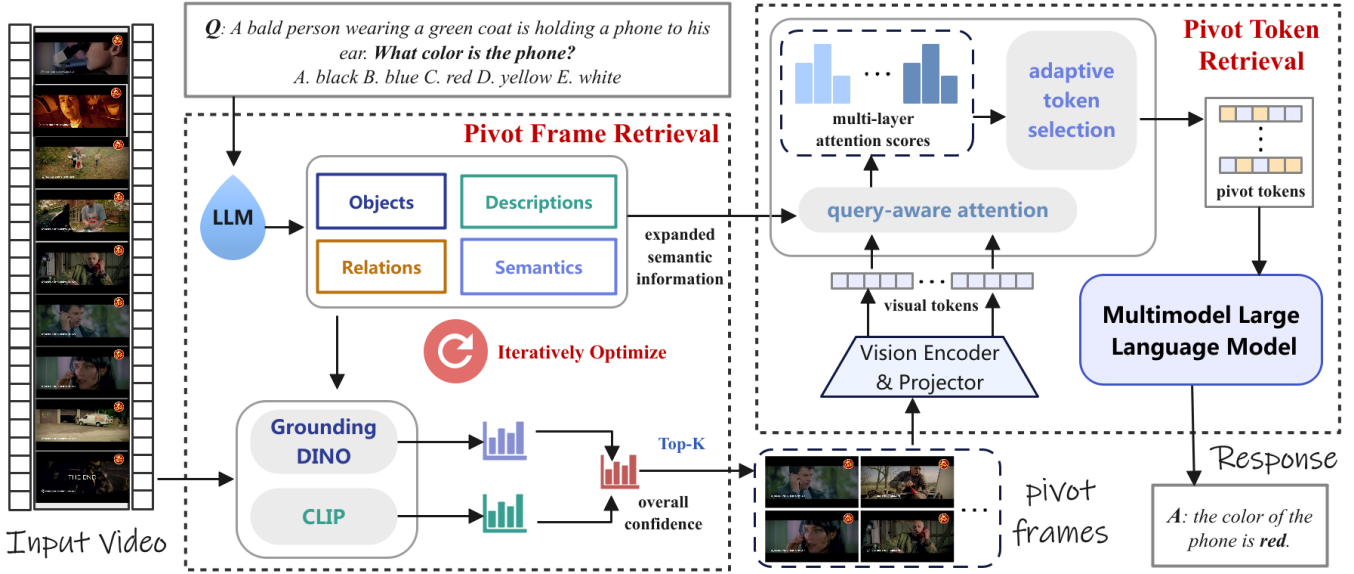


Figure 1: The overall framework of our proposed APVR. We integrate two plug-and-play components, Pivot Frame Retrieval and Pivot Token Retrieval, into MLLMs to improve the performance of long video understanding. APVR is training-free and provides a alternative to parameter scaling. With frame-level and token-level adaptive selection, it can accurately understand complex videos with computational efficiency.

aims to retrieve the most important information to feed into MLLM for the final response. To achieve this, we build two main components in APVR: *Pivot Frame Retrieval* (PFR) and *Pivot Token Retrieval* (PTR). In PFR, we design an efficient strategy to search pivot frames  $\mathcal{F}_{pivot} = \{f_t\}_{t=1}^K$  with expanded queries and basic visual models. In PTR, we explore an attention-driven token selection to retrieve pivot tokens  $\mathcal{T}_{pivot}$  that are most relevant with expanded queries. Finally, any type of MLLM can be integrated into our plug-and-play APVR to generate accurate response to the input video and query.

### 3.2 Pivot Frame Retrieval

We build an efficient algorithm to retrieve the pivot frames in an iterative manner. To be specific, we first expand the original query into four types of semantic information using LLM. The expanded information is then utilized for frame scoring using two basic visual models to obtain different types of confidence. Finally, all confidence is properly integrated to sort the video frames and select the top-K frames for the subsequent module.

**Semantic Information Expansion** To filter out the most relevant video frame only based on the brief query is challenging. Thus, we expand the given query  $Q$  to four types of semantic information as follows:

**Objects:** The key objects  $O_k$  or cue objects  $O_c$  that are detectable by visual models such as Grounding-DINO (e.g., "bold person", "phone", "blue background").

**Descriptions:** The entity or hypernym concepts of objects based on knowledge graph augmentation, denoted as  $D$ . (e.g. "pearl headband: decorative accessory worn on head; jewelry")

**Relations:** The triplet relationship  $R \subseteq O \times \mathcal{R} \times O$  to enhance the confidence of frames with logical links between objects. In each triplet  $(o_i, r, o_j)$ , the type of relation  $r \in \mathcal{R}$  is exactly one of the following: (1) **spatial** which means that  $o_i$  and  $o_j$  appear in the same frame such as "a bold man holding a red phone". (2) **time** which means that  $o_i$  and  $o_j$  appear in different frames in orders such as "A woman walks through, after a cat follows." (3) **attribute** which means that  $o_i$  appears with an attribute describable by  $o_j$  such as "A woman in a white skirt". (4) **causal** which means that  $o_i$  and  $o_j$  appear in orders with a cause-effect manner such as "A woman opens the door, the cat is scared and runs out."

**Semantics:** The semantics information of query and options based on knowledge graph, denoted as  $M$  (e.g., leash often appears with dog).

**Multi-modal Confidence Scoring** Given a video  $\mathcal{F}$  consisting of  $N$  frames, and a textual query  $Q$  with expanded semantic information  $\{O_k, O_c, D, R, M\}$ , instead of exhaustively processing all frames, we first uniformly sample few frames with stride  $\nabla$  in the first turn scoring and then adaptively resample frames for the subsequent iteration based on the online updated frame confidence.

Our algorithm exploits two basic visual models, i.e., Grounding-DINO and CLIP, to comprehensively score the confidence of video frames and iteratively optimize the overall confidence as follows:

**CLIP-based Similarity Scoring:** We leverage the CLIP model to compute cross-modal similarity between text and visual features. For each of the sampled frames  $\{f_t\}_{t=1}^{N_s}$ , we encode it using the CLIP image encoder  $\phi_I(\cdot)$ :

$$v_t = \frac{\phi_I(f_t)}{\|\phi_I(f_t)\|_2}. \quad (1)$$

The query as well as the expanded description and semantics are aggregated and encoded using the CLIP text encoder  $\phi_T(\cdot)$ :

$$t_{agg} = \sum_e \frac{\phi_T(e)}{\|\phi_T(e)\|_2}, e \in \{Q, D, M\}. \quad (2)$$

The CLIP similarity score for frame  $f_t$  is then calculated as:

$$s_t^{CLIP} = \text{softmax}(\tau \cdot v_t \cdot t_{agg}) \quad (3)$$

, where  $\tau$  is a temperature parameter set to 100 to sharpen the score distribution.

**Grounding-DINO Object Detection:** To enhance the retrieval precision with key/cue objects along with their relations, we first employ Grounding-DINO to identify extracted objects:

$$\mathcal{B}_t, \mathcal{L}_t = \Psi_{GD}(f_t, O_k \cup O_c) \quad (4)$$

, where  $\Psi(\cdot)$  is the Grounding-DINO model that returns bounding boxes  $\mathcal{B}_t$  and corresponding confidence logits  $\mathcal{L}_t$  for frame  $f_t$ . The score of detection is then computed as:

$$s_t^o = \text{softmax}(\max(\mathcal{L}_t)). \quad (5)$$

To further model the logic relations among objects in the same or different frames to enhance the detection results, we update the score by adding corresponding frame score if there are satisfied relation triplets in this frame as follows:

$$s_t^{GD} = s_t^o + \sum_r (\omega_r \cdot s_r) \quad (6)$$

, where  $r$  is exactly one of spatial/time/attribute/causal and  $\omega_r$  is the corresponding weight to control the contribution of each type of relation.

The final confidence score of this iteration is computed as a weighted sum of the CLIP and Grounding-DINO scores:

$$\mathcal{S}_t = (1 - \lambda) \cdot s_t^{CLIP} + \lambda \cdot s_t^{GD}. \quad (7)$$

**Temporal Diffusion and Adaptive Resampling** To account for the temporal continuity of video content and improve frame resampling, we introduce a temporal score diffusion mechanism that propagates confidence scores across neighboring frames. Specifically, for a scored frame  $t$ , we update the score distribution in a window:

$$\mathcal{S}_i = \max(\mathcal{S}_i, \frac{\mathcal{S}_t}{1 + |i - t|}), i \in [t - w, t + w] \quad (8)$$

This diffusion process ensures that frames adjacent to high-confidence frames receive boosted scores proportional to their proximity, which helps capture temporally coherent segments relevant to the query. The score distribution of the whole video  $\mathcal{S}$  is then updated. In addition, the frames scored in iteration  $p$  are marked as visited  $\{\epsilon_t = 1 \mid f_t \in \mathcal{F}_{vis}^p\}$ . Based on  $\mathcal{S}$ , we further design an adaptive and hybrid candidate sampling strategy for subsequent iterations that combines two types of set:

**High-confidence Set:** We select frames with higher scores from all unvisited frame set  $\mathcal{C}_t = \{f_t \mid \epsilon_t = 0\}_{t=1}^{N_c}$  based on the distribution as:

$$\mathcal{H}_t = \text{topk}(\mathcal{S} \odot \mathcal{C}_t), k = \frac{N}{2\nabla} \quad (9)$$

**Uncertainty Set:** We identify the regions with high Shannon entropy in the score distribution as:

$$\mathcal{E}_\gamma(s_i) = - \sum_{j=i-\gamma}^{i+\gamma} e_j \log(e_j), e_j = \frac{s_j}{\sum_{k=j-\gamma}^{j+\gamma} s_k} \quad (10)$$

, then the sampled frame is determined by:

$$\mathcal{U}_t = \{f_t \mid \mathcal{E}_\gamma(s_t) > \mu + 0.5\sigma\} \quad (11)$$

, where  $\mu$  and  $\sigma$  are the mean and standard deviation of entropy values across candidate set.

The final union candidate set is  $\mathcal{L}_t = \mathcal{H}_t \cup \mathcal{U}_t$ , which will be used for adaptive sampling. To ensure progressively finer sampling, we decrease the stride in each iteration by  $\nabla^p = \max(1, \frac{\nabla}{p+1})$ . The selected frames  $\mathcal{L}_{selected}$  for next iteration are sample in the way as:

$$\mathcal{L}_{selected} = L_* \cup L_{rand}, \quad (12)$$

$$L_* = \text{Multinomia}(\mathcal{S}_{\mathcal{L}_t}, (1 - \alpha)N_c), \quad (13)$$

$$L_{rand} = U(\text{Perm}(\alpha N_c)) \quad (14)$$

, where  $\alpha$  balances the score-based importance sampling  $L_*$  and the diverse random sampling  $L_{rand}$  to capture the full semantic content of the video and also avoid falling into local optimum.

After  $P$  iterations, the  $K$  pivot frames are retrieved by  $\mathcal{F}_{pivot} = \text{topk}(\mathcal{S} \odot \mathcal{F}) = \{f_t\}_{t=1}^K$  and fed into the next module.

### 3.3 Pivot Token Retrieval

Building upon the pivot frame selection mechanism, we propose a novel Pivot Token Retrieval framework that extends the concept of semantic importance from frame-level to token-level granularity. In this module, we adaptively retrieve the pivot visual token representations within the multi-modal language model to maintain computational efficiency while preserving critical semantic information.

First, the retrieved pivot frames  $\mathcal{F}_{pivot}$  are processed by a Vision Encoder  $\mathcal{G}(\cdot)$  and a Projector  $\mathcal{P}(\cdot)$  to generate dense visual token representations:  $\mathcal{T}_{visual} = \mathcal{G}(\mathcal{P}(\mathcal{F}_{pivot})) = \{\mathcal{T}_t \mid \mathcal{T}_t \in R^{e \times d_T}\}_{t=1}^K$ , where  $d_T$  denotes the number of tokens per frame. Our objective is to retrieve the pivot token  $\mathcal{T}_{pivot}$ . To this end, we introduce two components: query-aware multi-layer attention scoring and adaptive token selection.

**Query-aware Multi-Layer Attention Scoring** The core innovation lies in leveraging the expanded semantic information from the LLM-augmented query to guide token selection across multiple transformer layers. This process captures both local and global semantic relationships between the visual content and the textual query. The attention scores for layer  $l$  are computed as:

$$A_{cross}^{(l)} = \text{softmax}\left(\frac{q_{text}^{(l)} \cdot (k_{visual}^{(l)})^T}{\sqrt{d}}\right) \quad (15)$$

, where  $A_{cross}^{(l)} \in R^{B \times H \times d_q \times d_v}$ ,  $q_{text}$  denotes the query states derived from the expanded semantic information

Model	Params	Type	LongVideoBench		VideoMME		
			Val	Long	Medium	Short	Overall
<i>Proprietary Models</i>							
GPT4-V	-	training-based	59.1	53.5	-	-	59.9
GPT4-o	-	training-based	66.7	65.3	-	-	71.9
Gemini-1.5-Pro	-	training-based	64.0	67.4	-	-	75.0
<i>Open-Source MLLMs</i>							
VideoLLaVA(Lin et al. 2023)	7B	training-based	58.2	36.2	38.0	45.3	39.9
VITA-1.5(Fu et al. 2025)	7B	training-based	-	47.1	54.2	67.0	56.1
mPLUG-Owl3(Ye et al. 2024)	7B	training-based	52.1	50.1	57.7	70.0	59.3
VideoLLaMA3(Zhang et al. 2025)	7B	training-based	59.8	54.9	63.7	<b>80.1</b>	66.2
Oryx-1.5(Liu et al. 2024c)	7B	training-based	56.3	-	-	-	58.3
QuoTA(Luo et al. 2025)	7B	training-free	59.0	55.7	64.9	77.1	65.9
Video-XL(Shu et al. 2024)	7B	training-based	49.5	-	-	-	55.5
ViLaMP(Cheng et al. 2025a)	7B	training-based	57.8	-	-	-	67.5
AdaReTaKe(Wang et al. 2025a)	7B	training-free	62.6	58.3	-	-	67.7
AKS(Tang et al. 2025a)	7B	training-free	62.7	-	-	-	65.3
Kangaroo(Liu et al. 2024a)	8B	training-based	54.8	-	-	-	46.6
NVILA(Liu et al. 2024d)	8B	training-based	57.7	54.8	62.2	75.7	64.2
ByteVideoLLM(Wang et al. 2024a)	14B	training-based	-	56.4	62.9	74.4	64.6
Qwen2-VL(Wang et al. 2024b)	7B	training-based	55.6	53.8	-	-	63.3
Qwen2-VL w/ APVR(ours)	7B	training-free	60.9	55.1	66.2	73.9	65.2
Qwen2.5-VL(Bai et al. 2025b)	7B	training-based	59.5	55.6	-	-	65.4
Qwen2.5-VL w/ APVR(ours)	7B	training-free	<b>64.9</b>	<b>59.1</b>	<b>67.8</b>	78.3	<b>68.4</b>

Table 1: Video understanding accuracy(%) on LongVideoBench and VideoMME. The proposed APVR is applied upon two baseline MLLMs. The Methods are divided into two categories: training-based and training-free. APVR based on Qwen2.5-VL achieved state-of-the-art results on both the two benchmarks.

$\{Q, D, M\}$  and  $k_{visual}$  denotes the key states derived from the visual tokens  $\{\mathcal{T}_t\}_{t=1}^K$ . Then the token-level attention scores of each layer are aggregated at the query dimension:

$$a^{(l)} = \sum_{d_q} A_{cross}^{(l)} \quad (16)$$

This formulation captures how much attention each key token receives across all query positions, providing a comprehensive measure of its importance for the current layer’s computations.

**Adaptive Token Selection** The simplest token selection strategy is to directly retain the Top-K tokens while evicting others. However, this approach ignores the continuity of visual tokens and may reduce accuracy. Another factor that matters is that attention scores across heads may exist disparities, which further result in independence between heads. Thus, considering the continuity of visual tokens as well as the disparities across heads, we introduce an adaptive token selection strategy consisting of two components: dynamic chunk-wise selection and head-wise soft voting.

**Dynamic Chunk-wise Selection:** The long video understanding reaches the memory wall when prefilling the visual token. Thus, we perform token selection for the KV cache to reduce redundancy. Given a key or value cache to select, we first divide it into  $W$  chunks at the token dimension. Then,

the base selection ration of chunk  $w$  is computed as:

$$\eta_w^{(l)} = \frac{\sum_w a^{(l)}}{\max(\{\sum_w a^{(l)} \mid w = 1, \dots, W\})} \quad (17)$$

The dynamic ratio each chunk is calculated by:

$$\rho_w^{(l)} = \min(1.0, \sqrt{\frac{|\{j : a_j^{(l)} > 0.01 \cdot \max(a^{(l)})\}|}{L_w}}) \quad (18)$$

, where  $L_w$  is the chunk length. The final selection ratio is determined by:

$$\gamma_w^{(l)} = \eta_w^{(l)} \cdot \rho_w^{(l)} \quad (19)$$

**Head-wise Soft Voting** Based on the ratio, we can select pivot token in each chunk by:

$$\mathcal{Z}_w^{(l)} = \text{topk}(a_w^{(l)}, k = \gamma_w^{(l)} \cdot L_w) \quad (20)$$

This results may appear significant disparities in different attention heads. To figure this, we introduce a head-wise voting for final token selection:

$$\mathcal{Z}_w^{(l)} = \text{topk}(\sum_{j=1}^h \text{softmax}(a_{w,j}^{(l)}), k = \gamma_w^{(l)} \cdot L_w) \quad (21)$$

, where the softmax function calculate the per-head scores and give a soft voting via normalization and sum. Finally, we update the KV cache as selected pivot token in each layer:

$$\mathcal{T}_{pivot}^{(l)} = \text{Concat}(\{\mathcal{Z}_w^{(l)}\}_{w=1}^W) \quad (22)$$

**Query:** In the room on the screen, there is a man wearing green clothes with a beard. Behind him, there is a white cabinet and a wooden shelf. On the shelf, there is a black bag. What did the man in the video do upon entering the scene?

**Expanded Semantic Information:**

"key\_objects": [{"man", "white cabinet", "wooden shelf", "black bag"}]  
 "cue\_objects": [{"green clothes", "beard", "right hand", "left hand"}]  
 "relations": [{"man", "Attribute", "green clothes"}, {"wooden shelf", "Spatial", "black bag"}]  
 "descriptions": [{"beard": [{"facial hair feature on man"}]}  
 "semantics": [{"right hand and left hand are body parts used for touching or carrying objects"}]

**Retrieved Pivot Frames:**



**Qwen2.5-VL:**  
**B. Touched his beard with his right hand**

**Qwen2.5-VL w/ APVR:**  
**D. Touched his beard with his left hand**

**Query:** In a white room, a man wearing a dark blue jacket is speaking on screen. There is a black microphone in front of him, he has dark skin, and he is sporting a beard. A black map is hanging on the wall behind him, there is a whiteboard on the left side of the screen, and on the right side, there is another wall with a black-bordered paper on it. What changes occur to this man's position on the screen when the 'Quiz Time 3' title, featuring many horizontal grids with black letters, appears?

**Expanded Semantic Information:**

"key\_objects": [{"man", "microphone", "map"}]  
 "cue\_objects": [{"whiteboard", "black-bordered paper", "Quiz Time 3 title"}]  
 "relations": [{"man", "Spatial", "microphone"}, {"Quiz Time 3 title", "Time", "man"}, {"wooden shelf", "Spatial", "black bag"}]  
 "descriptions": [{"microphone": [{"device for amplifying sound; positioned in front of man"}]}  
 "semantics": [{"titles may reposition subjects to maintain visibility"}]

**Retrieved Pivot Frames:**



**Qwen2.5-VL:**  
**C. The man's position on the screen shifts to the bottom-left corner.**

**Qwen2.5-VL w/ APVR:**  
**D. The man's position on the screen shifts to the bottom-right corner.**

**Query:** On the surface of the sink are a toothbrush and toothpaste. Reflected in the glass above the sink is a man wearing a white hat and a white short-sleeved shirt, holding a camera. What changes when this man appears in the driver's seat?

**Expanded Semantic Information:**

"key\_objects": [{"man", "white hat", "white short-sleeved shirt", "camera"}]  
 "cue\_objects": [{"sink", "toothbrush", "toothpaste", "driver's seat"}]  
 "relations": [{"man", "Attribute", "white hat"}, {"man", "Attribute", "white short-sleeved shirt"}, {"man", "Spatial", "camera"}]  
 "descriptions": [{"white hat": [{"headwear worn by the man; protective or decorative headgear"}]}  
 "semantics": [{"driver's seat implies a vehicle context"}]

**Retrieved Pivot Frames:**



**Qwen2.5-VL:**  
**E. He changed to a gray long-sleeved coat**

**Qwen2.5-VL w/ APVR:**  
**B. He changed to a black long-sleeved coat**

**Query:** The video shows the interior of a museum with two white light fixtures. Many white cabinets containing different artifacts are placed on the dark-colored floor. On the right side of the screen, a woman is sitting in a room illuminated by white lights, shown in a small video frame. What material is the protective cover placed over the artifacts on the cabinet made of?

**Expanded Semantic Information:**

"key\_objects": [{"white light fixtures", "white cabinets", "artifacts"}]  
 "cue\_objects": [{"protective cover", "dark-colored floor", "woman in illuminated room"}]  
 "relations": [{"white cabinets", "Spatial", "protective cover"}]  
 "descriptions": [{"protective cover": [{"transparent material; artifact protection device"}]}  
 "semantics": [{"protective covers are often made of glass or acrylic for artifact preservation", "glass is commonly used in museums due to its transparency and durability"}]

**Retrieved Pivot Frames:**



**Qwen2.5-VL:**  
**E. Acrylic**

**Qwen2.5-VL w/ APVR:**  
**C. Glass**

Figure 2: Qualitative Comparison of APVR with the baseline MLLM. The expanded semantic information is significant complementary for pivot frame retrieval. The number and score of the pivot frame is drawn in the left-top with green and red text, respectively. Yellow stars indicate the key frame for answering the question. Green answer represents correct while red one represents wrong.

Finally, the selected pivot tokens will be fed into a MLLM to generate the final response.

## 4 Experiments

### 4.1 Experimental setup

**Datasets** We evaluate the performance of APVR in two popular benchmarks that contains hour-level videos: **LongVideoBench** (Wu et al. 2024). A benchmark for long-context video understanding, consisting of 3,763 videos with 6,678 annotated multiple-choice questions across 17 categories of referred reasoning questions. It evaluates models across temporal reasoning, character tracking, and narrative understanding, making it particularly well-suited for evaluating APVR’s dual-granularity retrieval mechanisms in processing hour-long video content. **VideoMME** (Fu et al. 2024). A multi-modal evaluation benchmark focused on fine-grained video understanding tasks requiring precise visual-textual alignment and detailed semantic comprehension. It comprises 900 videos totaling 256 hours, with 2,700 manually labeled complex multiple-choice question-answer pairs across 30 subfields. It’s emphasis on both coarse-grained temporal understanding and fine-grained semantic detail extraction aligns precisely with APVR’s hierarchical information retrieval strategy. To highlight the importance of the pivot information retrieval for visual understanding, we do not use video subtitles for the two benchmarks.

**Implementation Details** We integrate APVR with two baseline MLLMs, namely, Qwen2-VL-7B (Wang et al. 2024b) and Qwen2.5-VL-7B (Bai et al. 2025b). The MLLMs process a prompt involving the question, retrieved pivot video frames, and the multi-choice answer options to generate responses. We first densely extracted the raw frames from video at 2 fps. Then, the sampled frames are iteratively scored using two basic visual models: CLIP (Radford et al. 2021) with ViT-B-16 (Dosovitskiy et al. 2020) backbone, and Grounding-DINO (Liu et al. 2024b) with Swin-T (Liu et al. 2021) backbone, based on the expanded semantic information generated by LLM. The prompt for query expansion is in the supplementary materials. All evaluations are conducted on 8 NVIDIA A800 GPUs with 80GB memory, using LMMs-Eval (Zhang et al. 2024a) framework. Our APVR enables processing of up to 1024 frames, compared to the baseline 7B model’s capacity of 256 frames under optimal MLLM configurations.

### 4.2 Comparison to the State-of-the-Art

**Quantitative results** We first compare the accuracy of video question answering between APVR with recent training-based or training-free methods. Results are summarized in Table 1. Upon baseline of Qwen2-VL, APVR improves the overall accuracy by 9.5% and 3.0% in LongVideoBench and VideoMME, respectively. Upon a stronger baseline Qwen2.5-VL, our APVR also improves

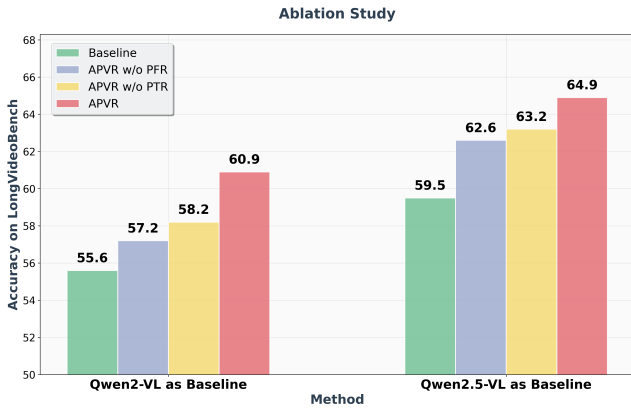


Figure 3: The result of ablation study on LongVideoBench for the two designed components: PFR and PTR.

the overall accuracy by 8.3% in LongVideoBench and 4.6% in VideoMME, respectively. Notably, APVR based on Qwen2.5-VL reaches 64.9 accuracy in LongVideoBench, which is higher than the powerful proprietary models such as GPT4-V and Gemini-1.5-Pro. The overall performance of APVR also surpasses other training-based and training-free methods with larger parameter scales such as 8B and 14B. Another notable result is that our APVR reaches highest accuracy on long and medium video samples of VideoMME, which demonstrates that our dual-granularity retrieval significantly assist capturing the most important information from extra-long videos and then improve the performance.

**Qualitative results** In Figure 2, we illustrate representative video understanding results of APVR and the baseline Qwen2.5-VL, over four samples with hour-level video. First, it can be seen that the expanded semantic information significantly supplement various reference needed by subsequent retrieval. Next, it can be observed that the retrieved pivot frames are closely related to the query and the expanded semantic information. However, in many videos, there are many frames which are similar and all related to the text. Based on the frame score distribution, if we select only a few frames, the most pivot frames may be lost. Otherwise, if we select too many frames such as 1024 frames, we will face the memory wall. Based on APVR, one can select 1024 frames and then compress the visual token via our pivot token retrieval. As a result, MLLMs can get a comprehensive view of adequate and pivot content, and thus obtain the correct answer.

### 4.3 Ablation Studies

**Ablation studies on PFR and PTR** To prove the effectiveness of the two proposed components in APVR, we conduct an ablation study for PFR and PTR in LongVideoBench. The results are illustrated in Figure 3. It can be seen that, based on two different baseline MLLMs, the accuracies of APVR decline without both PFR and PTR. These results significantly demonstrate the rationality and validity of the designed dual-granularity pivot information retrieval strategy.

$k$	Long	Average	$\lambda$	Long	Average
1024	58.3	64.9	0.1	57.4	64.2
256	56.4	63.1	0.2	57.8	64.5
128	53.0	61.1	0.5	58.3	64.9
64	49.8	58.6	0.8	58.0	64.8
32	45.4	54.3	0.9	58.9	64.5

Table 2: Ablations of retained frame number and weight for scoring models.

$p$	$\nabla$	Long	Medium	Short	Average
3	2	56.4	62.1	77.3	62.9
3	4	58.3	65.8	77.3	64.9
3	8	55.1	64.6	77.3	63.1
2	4	56.0	66.0	77.3	63.9
4	4	58.0	65.8	77.3	64.7
5	4	58.5	64.5	77.3	64.5

Table 3: Ablations of iteration number and the initial sample stride.

**Ablation studies on other hyper-parameters** First, we study the impact of retained frame number  $k$  and the weight  $\lambda$  of the two visual models for frame scoring. Results are summarized in Table 2. The ablation studies are conducted on LongVideoBench. It can be seen that the larger the frame number, the better the performance. This trend is similar in accuracy of all videos or long videos. For  $\lambda$ , we find that the best performance is achieved when we set a trade-off between the CLIP and Grounding-DINO model.

Second, we ablation the best setting of the core hyper-parameters, i.e., the iteration time  $p$  and the initial sample stride  $\nabla$  in the first iteration. It can be observed that the best performance is achieved when  $p = 3$  and  $\nabla = 4$ . The accuracies of samples with long and medium videos decrease when  $p$  and  $\nabla$  are changed. This is because the adaptive frame scoring needs to maintain a balance between sampling and distribution update.

## 5 Conclusion

We present APVR, a training-free framework that addresses the fundamental memory wall limitation in hour-level video understanding through adaptive hierarchical information retrieval. The framework’s dual-granularity approach, combining Pivot Frame Retrieval with Pivot Token Retrieval, enables processing of extensive video sequences while maintaining computational tractability and semantic accuracy. Experimental validation demonstrates substantial performance improvements across standard benchmarks, with APVR-enhanced models achieving state-of-the-art results among training-free approaches. The framework’s plug-and-play architecture ensures immediate deployment compatibility with existing MLLM systems without requiring expensive retraining procedures. This paradigm shift toward retrieval-based optimization provides a sustainable alternative to parameter scaling or extensive training.

## References

- Bai, S.; Chen, K.; Liu, X.; Wang, J.; Ge, W.; Song, S.; Dang, K.; Wang, P.; Wang, S.; Tang, J.; et al. 2025a. Qwen2. 5-vl technical report. *arXiv preprint arXiv:2502.13923*.
- Bai, S.; Chen, K.; Liu, X.; Wang, J.; Ge, W.; Song, S.; Dang, K.; Wang, P.; Wang, S.; Tang, J.; et al. 2025b. Qwen2. 5-vl technical report. *arXiv preprint arXiv:2502.13923*.
- Chen, Y.; Xue, F.; Li, D.; Hu, Q.; Zhu, L.; Li, X.; Fang, Y.; Tang, H.; Yang, S.; Liu, Z.; et al. 2024. Longvila: Scaling long-context visual language models for long videos. *arXiv preprint arXiv:2408.10188*.
- Cheng, C.; Guan, J.; Wu, W.; and Yan, R. 2025a. Scaling Video-Language Models to 10K Frames via Hierarchical Differential Distillation. *arXiv preprint arXiv:2504.02438*.
- Cheng, C.; Guan, J.; Wu, W.; and Yan, R. 2025b. Scaling Video-Language Models to 10K Frames via Hierarchical Differential Distillation. *arXiv preprint arXiv:2504.02438*.
- Dosovitskiy, A.; Beyer, L.; Kolesnikov, A.; Weissenborn, D.; Zhai, X.; Unterthiner, T.; Dehghani, M.; Minderer, M.; Heigold, G.; Gelly, S.; et al. 2020. An image is worth 16x16 words: Transformers for image recognition at scale. *arXiv preprint arXiv:2010.11929*.
- Fu, C.; Dai, Y.; Luo, Y.; Li, L.; Ren, S.; Zhang, R.; Wang, Z.; Zhou, C.; Shen, Y.; Zhang, M.; et al. 2024. Videomme: The first-ever comprehensive evaluation benchmark of multi-modal llms in video analysis. *arXiv preprint arXiv:2405.21075*.
- Fu, C.; Lin, H.; Wang, X.; Zhang, Y.-F.; Shen, Y.; Liu, X.; Cao, H.; Long, Z.; Gao, H.; Li, K.; et al. 2025. Vita-1.5: Towards gpt-4o level real-time vision and speech interaction. *arXiv preprint arXiv:2501.01957*.
- Guo, W.; Chen, Z.; Wang, S.; He, J.; Xu, Y.; Ye, J.; Sun, Y.; and Xiong, H. 2025. Logic-in-Frames: Dynamic Keyframe Search via Visual Semantic-Logical Verification for Long Video Understanding. *arXiv preprint arXiv:2503.13139*.
- Li, K.; Li, X.; Wang, Y.; He, Y.; Wang, Y.; Wang, L.; and Qiao, Y. 2024a. Videomamba: State space model for efficient video understanding. In *European Conference on Computer Vision*, 237–255. Springer.
- Li, X.; Wang, Y.; Yu, J.; Zeng, X.; Zhu, Y.; Huang, H.; Gao, J.; Li, K.; He, Y.; Wang, C.; et al. 2024b. Videochat-flash: Hierarchical compression for long-context video modeling. *arXiv preprint arXiv:2501.00574*.
- Lin, B.; Ye, Y.; Zhu, B.; Cui, J.; Ning, M.; Jin, P.; and Yuan, L. 2023. Video-llava: Learning united visual representation by alignment before projection. *arXiv preprint arXiv:2311.10122*.
- Liu, J.; Wang, Y.; Ma, H.; Wu, X.; Ma, X.; Wei, X.; Jiao, J.; Wu, E.; and Hu, J. 2024a. Kangaroo: A powerful video-language model supporting long-context video input. *arXiv preprint arXiv:2408.15542*.
- Liu, S.; Zeng, Z.; Ren, T.; Li, F.; Zhang, H.; Yang, J.; Jiang, Q.; Li, C.; Yang, J.; Su, H.; et al. 2024b. Grounding dino: Marrying dino with grounded pre-training for open-set object detection. In *European Conference on Computer Vision*, 38–55. Springer.
- Liu, X.; Shu, Y.; Liu, Z.; Li, A.; Tian, Y.; and Zhao, B. 2025a. Video-XL-Pro: Reconstructive Token Compression for Extremely Long Video Understanding. *arXiv preprint arXiv:2503.18478*.
- Liu, Y.; Lin, K. Q.; Chen, C. W.; and Shou, M. Z. 2025b. VideoMind: A Chain-of-LoRA Agent for Long Video Reasoning. *arXiv preprint arXiv:2503.13444*.
- Liu, Z.; Dong, Y.; Liu, Z.; Hu, W.; Lu, J.; and Rao, Y. 2024c. Oryx mllm: On-demand spatial-temporal understanding at arbitrary resolution. *arXiv preprint arXiv:2409.12961*.
- Liu, Z.; Lin, Y.; Cao, Y.; Hu, H.; Wei, Y.; Zhang, Z.; Lin, S.; and Guo, B. 2021. Swin transformer: Hierarchical vision transformer using shifted windows. In *Proceedings of the IEEE/CVF international conference on computer vision*, 10012–10022.
- Liu, Z.; Zhu, L.; Shi, B.; Zhang, Z.; Lou, Y.; Yang, S.; Xi, H.; Cao, S.; Gu, Y.; Li, D.; et al. 2024d. NVILA: Efficient frontier visual language models. *arXiv preprint arXiv:2412.04468*.
- Luo, Y.; Chen, W.; Zheng, X.; Huang, W.; Yin, S.; Lin, H.; Fu, C.; Huang, J.; Ji, J.; Luo, J.; et al. 2025. QuoTA: Query-oriented Token Assignment via CoT Query Decouple for Long Video Comprehension. *arXiv preprint arXiv:2503.08689*.
- Park, J.; Ranasinghe, K.; Kahatapitiya, K.; Ryu, W.; Kim, D.; and Ryoo, M. S. 2024. Too many frames, not all useful: Efficient strategies for long-form video qa. *arXiv preprint arXiv:2406.09396*.
- Radford, A.; Kim, J. W.; Hallacy, C.; Ramesh, A.; Goh, G.; Agarwal, S.; Sastry, G.; Askell, A.; Mishkin, P.; Clark, J.; et al. 2021. Learning transferable visual models from natural language supervision. In *International conference on machine learning*, 8748–8763. PmLR.
- Shen, X.; Xiong, Y.; Zhao, C.; Wu, L.; Chen, J.; Zhu, C.; Liu, Z.; Xiao, F.; Varadarajan, B.; Bordes, F.; et al. 2024. Longvu: Spatiotemporal adaptive compression for long video-language understanding. *arXiv preprint arXiv:2410.17434*.
- Shen, Y.; Fu, C.; Dong, S.; Wang, X.; Chen, P.; Zhang, M.; Cao, H.; Li, K.; Zheng, X.; Zhang, Y.; et al. 2025. Long-VITA: Scaling Large Multi-modal Models to 1 Million Tokens with Leading Short-Context Accuracy. *arXiv preprint arXiv:2502.05177*.
- Shu, Y.; Liu, Z.; Zhang, P.; Qin, M.; Zhou, J.; Liang, Z.; Huang, T.; and Zhao, B. 2024. Video-xl: Extra-long vision language model for hour-scale video understanding. *arXiv preprint arXiv:2409.14485*.
- Song, E.; Chai, W.; Wang, G.; Zhang, Y.; Zhou, H.; Wu, F.; Chi, H.; Guo, X.; Ye, T.; Zhang, Y.; et al. 2024. Moviechat: From dense token to sparse memory for long video understanding. In *Proceedings of the IEEE/CVF Conference on Computer Vision and Pattern Recognition*, 18221–18232.
- Su, J.; Ahmed, M.; Lu, Y.; Pan, S.; Bo, W.; and Liu, Y. 2024. Roformer: Enhanced transformer with rotary position embedding. *Neurocomputing*, 568: 127063.

Tang, X.; Qiu, J.; Xie, L.; Tian, Y.; Jiao, J.; and Ye, Q. 2025a. Adaptive Keyframe Sampling for Long Video Understanding. *arXiv preprint arXiv:2502.21271*.

Tang, X.; Qiu, J.; Xie, L.; Tian, Y.; Jiao, J.; and Ye, Q. 2025b. Adaptive Keyframe Sampling for Long Video Understanding. *arXiv preprint arXiv:2502.21271*.

Wang, H.; Nie, Y.; Ye, Y.; GuanYu, D.; Wang, Y.; Li, S.; Yu, H.; Lu, J.; and Huang, C. 2024a. Dynamic-VLM: Simple Dynamic Visual Token Compression for VideoLLM. *arXiv preprint arXiv:2412.09530*.

Wang, P.; Bai, S.; Tan, S.; Wang, S.; Fan, Z.; Bai, J.; Chen, K.; Liu, X.; Wang, J.; Ge, W.; et al. 2024b. Qwen2-vl: Enhancing vision-language model's perception of the world at any resolution. *arXiv preprint arXiv:2409.12191*.

Wang, X.; Si, Q.; Wu, J.; Zhu, S.; Cao, L.; and Nie, L. 2025a. AdaRETAKE: Adaptive Redundancy Reduction to Perceive Longer for Video-language Understanding. *arXiv preprint arXiv:2503.12559*.

Wang, X.; Zhang, Y.; Zohar, O.; and Yeung-Levy, S. 2024c. Videoagent: Long-form video understanding with large language model as agent. In *European Conference on Computer Vision*, 58–76. Springer.

Wang, Y.; Li, X.; Yan, Z.; He, Y.; Yu, J.; Zeng, X.; Wang, C.; Ma, C.; Huang, H.; Gao, J.; et al. 2025b. InternVideo2.5: Empowering Video MLLMs with Long and Rich Context Modeling. *arXiv preprint arXiv:2501.12386*.

Wei, X.; Liu, X.; Zang, Y.; Dong, X.; Zhang, P.; Cao, Y.; Tong, J.; Duan, H.; Guo, Q.; Wang, J.; et al. 2025. VideoRoPE: What Makes for Good Video Rotary Position Embedding? *arXiv preprint arXiv:2502.05173*.

Wu, H.; Li, D.; Chen, B.; and Li, J. 2024. Longvideobench: A benchmark for long-context interleaved video-language understanding. *Advances in Neural Information Processing Systems*, 37: 28828–28857.

Ye, J.; Wang, Z.; Sun, H.; Chandrasegaran, K.; Durante, Z.; Eyzaguirre, C.; Bisk, Y.; Niebles, J. C.; Adeli, E.; Fei-Fei, L.; et al. 2025. Re-thinking Temporal Search for Long-Form Video Understanding. *arXiv preprint arXiv:2504.02259*.

Ye, J.; Xu, H.; Liu, H.; Hu, A.; Yan, M.; Qian, Q.; Zhang, J.; Huang, F.; and Zhou, J. 2024. mplug-owl3: Towards long image-sequence understanding in multi-modal large language models. *arXiv preprint arXiv:2408.04840*.

Zhang, B.; Li, K.; Cheng, Z.; Hu, Z.; Yuan, Y.; Chen, G.; Leng, S.; Jiang, Y.; Zhang, H.; Li, X.; et al. 2025. VideoLLaMA 3: Frontier Multimodal Foundation Models for Image and Video Understanding. *arXiv preprint arXiv:2501.13106*.

Zhang, K.; Li, B.; Zhang, P.; Pu, F.; Cahyono, J. A.; Hu, K.; Liu, S.; Zhang, Y.; Yang, J.; Li, C.; et al. 2024a. Lmms-eval: Reality check on the evaluation of large multimodal models. *arXiv preprint arXiv:2407.12772*.

Zhang, P.; Zhang, K.; Li, B.; Zeng, G.; Yang, J.; Zhang, Y.; Wang, Z.; Tan, H.; Li, C.; and Liu, Z. 2024b. Long context transfer from language to vision. *arXiv preprint arXiv:2406.16852*.